

PREPARATION AND CHARACTERIZATION OF $\text{Cu}_2\text{CrSnS}_4$ THIN FILMS DEPOSITED AT DIFFERENT TEMPERATURES[†]

 Huda Talib^{a,b},  Nabeel A. Bakr^{a*},  Mohammed A. Abed^b

^aDepartment of Physics, College of Science, University of Diyala, Diyala, Iraq

^bDiyala General Directorate of Education, Diyala, Iraq

*Corresponding Author: nabeelalibakr@yahoo.com

Received October 6, 2022; revised November 12, 2022; accepted November 17, 2022

In this study, $\text{Cu}_2\text{CrSnS}_4$ thin films are prepared using chemical pyrolysis technique at various deposition temperatures (200, 250, 300, 350, 400 and 450 °C) and without any annealing process. The structure characteristics of the films have been studied by X ray diffraction (XRD), micro-Raman spectroscopy, and Field Emission Scanning Electron Microscope (FESEM), while the optical characteristics are investigated by UV-Visible spectrophotometry, and the electrical properties are described by Hall Effect test. Results of XRD for $\text{Cu}_2\text{CrSnS}_4$ (CCTS) films showed the tetragonal crystal structure of stannite phase with (112) preferred orientation. The results of Raman spectroscopy of the prepared CCTS thin films showed a clear peak at $\sim 336 \text{ cm}^{-1}$. Furthermore, the morphology results and through (FESEM) images of thin films surface showed different forms and shapes with different granular size ranging from 40 to 294 nm. Optical examination of the ultraviolet-visible spectrum showed an optical energy gap of (1.69-1.59 eV) which are considered to be suitable for thin films solar cells applications. The electrical measurements through Hall Effect test showed that the films have charge carriers of (p-type). From results analysis, the optimized temperature of the prepared (CCTS) samples was 350 °C.

Keywords: $\text{Cu}_2\text{CrSnS}_4$, Spray pyrolysis, Deposition temperature, XRD analysis, UV-Visible Spectroscopy, Hall Effect.

PACS: 88.40.jn; 73.61.-r; 81.15.Rs; 61.82.Fk; 78.20.-e

Due to the high values of absorption coefficient with suitable energy gap, the chalcogenides based on Cu showed promised future as effective materials for various applications. [1]. $\text{Cu}_2\text{CrSnS}_4$ (CCTS) material is interesting thanks to its positive characteristics for different optoelectronic applications [2, 3]. There are different techniques which can be used to deposit thin films of these types of materials such as chemical and physical methods. The spray pyrolysis method has many benefits such as that it is a cost-effective technique which does not need expensive and complicated parts and it is safe and friendly technique [4]. Many reports on the preparation of quaternary chalcogenide films were carried out by this method. Khodair et al. succeeded in preparing CZTS thin films [5]. Abed et al. deposited $\text{Cu}_2\text{FeSnS}_4$ films on soda-lime slides at different temperatures by the same technique [6]. The goal of this study is the investigation of preparation temperature impact on the structure and the optical, as well as the electronic characteristics of CCTS thin films prepared using spray pyrolysis method and to get good quality and homogeneous samples which are desirable as solar cell absorber layer.

EXPERIMENTAL PROCEDURE

The solution used to deposit the $\text{Cu}_2\text{CrSnS}_4$ (CCTS) films deposition has been prepared by dissolving 0.01 M of copper acetate monohydrate ($\text{Cu}(\text{CH}_3\text{COO})_2\cdot\text{H}_2\text{O}$) (Thomas Baker), 0.005 M of chromium chloride hexahydrate ($\text{CrCl}_3\cdot 6\text{H}_2\text{O}$) (Central Drug House), 0.005 M of tin chloride ($\text{SnCl}_2\cdot 2\text{H}_2\text{O}$) (Thomas Baker), and 0.004 M of thiocarbamide ($\text{SC}(\text{NH}_2)_2$) (BDH Chemicals Ltd.) in 0.1 l of distilled water. The concentration of thiocarbamide used is doubled to overcome the evaporation process. The detailed procedure is reported elsewhere [7].

RESULTS AND DISCUSSION

The XRD patterns of the deposited CCTS films at different substrate temperatures (200-450°C) and thickness of 300 nm are displayed in Figure 1. The patterns have clear peaks at 28.42°, 47.26° and 56.12° attributed to 112, 220 and 312 planes respectively which belong to the stannite tetragonal phase of CCTS material [8]. From the figure, it can be seen that there are no other peaks belonging to ternary and binary materials [9,10]. The standard card (00-031-0462) of the compound copper iron zinc tin sulfide ($\text{Cu}_4\text{FeZnSnS}_8$) was adopted for matching the present XRD patterns due to the lack of entries in the database of the International Center for Diffraction Data (ICDD) for the quaternary compound ($\text{Cu}_2\text{CrSnS}_4$) which we are investigating in this study, as the replacement of Zn in the quaternary compound ($\text{Cu}_2\text{ZnSnS}_4$) with near transition elements (e.g., Cr, Ni, Mn, Fe, Co, Fe, Mn) presents defects which are similar to ($\text{Cu}_2\text{ZnSnS}_4$) because their ionic radii vary slightly and thus no significant change in the crystal structure [11,12]. Table (1) depicts the XRD results of the (112) plane.

The inter-planar distance (d) was estimated by using Bragg formula [13]:

$$m\lambda = 2d\sin\theta, \quad (1)$$

where m is the diffraction order, θ is the angle of Bragg, and λ is the x-ray wavelength.

[†] Cite as: H. Talib, N.A. Bakr, and M.A. Abed, East Eur. J. Phys. 4, 183 (2022), <https://doi.org/10.26565/2312-4334-2022-4-19>

© H. Talib, N.A. Bakr, M.A. Abed, 2022

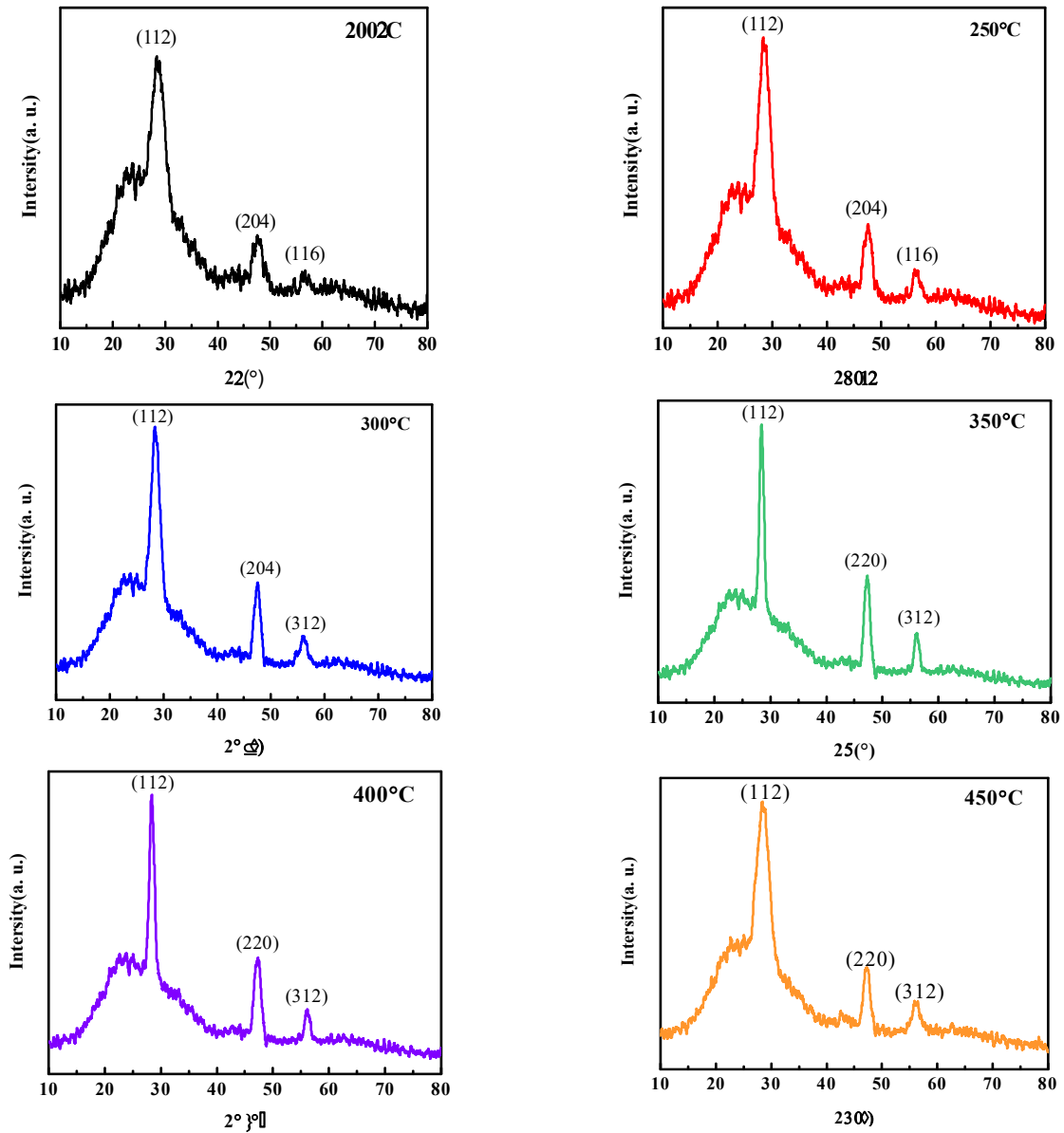


Figure 1. XRD patterns of CCTS samples at various temperatures.

Table 1. XRD results of CCTS films deposited at various temperatures

Deposition Temperature (°C)	2θ (°)	Inter-planar distance (Å)	Crystallite size (nm)	Texture coefficient
200	28.52	3.127	2.712	0.55
250	28.5	3.129	3.061	3.48
300	28.44	3.135	4.123	0.64
350	28.42	3.137	8.518	0.51
400	28.38	3.142	8.102	0.54
450	28.42	3.137	3.093	0.58

The lattice parameters are calculated through the well-known formula [8]:

$$\frac{1}{d^2} = \frac{h^2+k^2}{a^2} + \frac{l^2}{c^2} \tag{2}$$

where (h, k, l) represent indices of Miller; and the tetragonal unit cell parameters are represented by a and c.

The estimated values of a and c are a = 5.445 Å and c = 10.755 Å very near to the ideal ones a = 5.449 Å and c = 10.75 Å. The crystallite size (D) is estimated using the specifications of the peak corresponding to the (112) plane by Scherrer’s equation [14]:

$$D = \frac{k\lambda}{\beta \cos \theta} \tag{3}$$

where k = 0.9 and β is (FWHM) in radians.

The estimated values of (D) are shown in Table 1 which shows that when the temperature increases, the values of (D) increase up to 350 °C and then start to decrease.

This is owing to the high evaporation of the sprayed drops once this temperature has been reached, that is larger than that required to produce maximal pyrolysis and crystallization of the films, due to the high thermal energy. Thus, the crystallization mechanism is not complete [15]. Texture coefficient (T_c) is evaluated by the equation below [14]:

$$T_C = \frac{I_{(hkl)}/I^0_{(hkl)}}{N^{-1} \sum N I_{(hkl)}/I^0_{(hkl)}}, \quad (4)$$

where N stands for the number of peaks visible in XRD patterns, $I_{(hkl)}$ is the experimental relative intensity and $I^0_{(hkl)}$ is the ideal intensity.

T_c values for the prevailing direction of growth are listed in Table 1. T_c less than 1 values indicate that all films are polycrystalline. X-ray diffraction could be used to classify the materials phase, but it was difficult to distinguish between them because of how similar their compositions are. So, Raman spectroscopy at room temperature was performed and its results are plotted Figure 2 and Table 2 where the measured spectrum is plotted in black color, the green color represents the peaks resulting from the analysis of the measured spectra, and the sum of these peaks appears in red color representing the calculated spectrum, which is highly consistent with the measured black color.

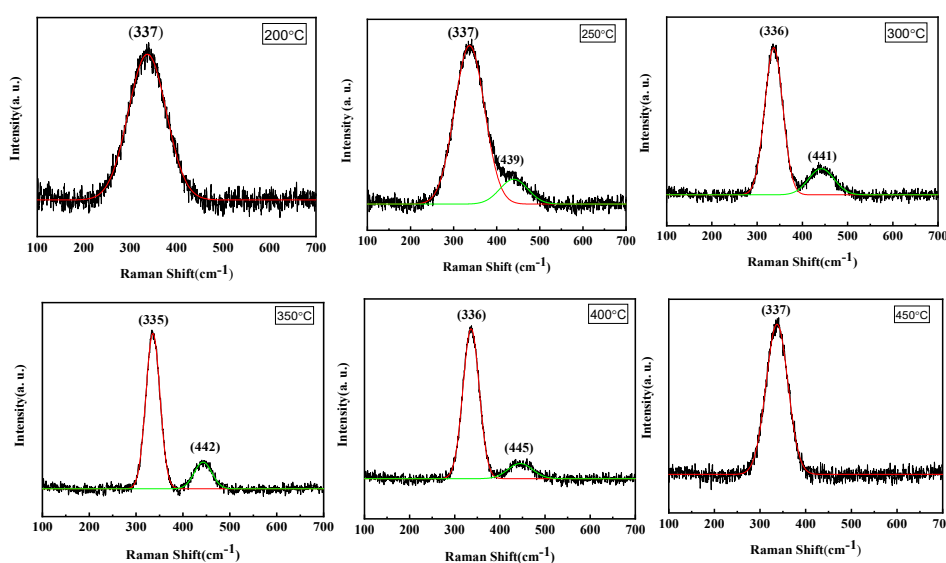


Figure 2. Micro-Raman shift of CCTS samples at various temperatures

Table 2. Result of micro-Raman spectra analysis of CCTS prepared in the current study

Temperature (°C)	Center of peak (cm ⁻¹)	Width of peak (cm ⁻¹)	Intensity (arb. u.)
200	337	81.574	4.989
250	337	69.424	6.007
	439	65.323	0.942
300	336	39.829	7.054
	441	56.592	1.252
350	335	29.986	7.987
	442	37.444	1.369
400	336	36.020	7.500
	445	54.428	0.759
450	337	47.999	7.029

Due to sulfur atoms vibrations in the CCTS structure, the prominent peaks of great intensity at the positions (335, 336, and 337 cm⁻¹) could be seen. This is consistent with the findings of other published investigations [16-18]. Other observed lower intensity peaks can be observed at (439, 441, 442, 445 cm⁻¹) which are consistent with the results of Yan et al. [18]. The surface topography of the films was imaged by FESEM. Figure 3 shows the micro-images at magnification of 50 Kx of the prepared CCTS films. At temperature (200, 250 °C), an irregular formation process appears with voids and cracks on the surface, and ball-like shapes begin to stick and align, with some temperature increasing, at (300 °C) we notice irregular distribution of nano-paper-like shapes with cracks and hole, and this indicates the formation of a new layer that starts to appear more on the surface and the emergence of a series of small particles in some areas that start to disappear when the substrate temperature increases. At 350, 400, and 450 °C substrate temperatures, we notice

cauliflower-like shapes having polyhedral forms, irregular distribution, and uneven growth, including some cracks and voids caused by crystal flaws, as well as secondary growth on the surface. This can be explained by the development of a new layer before the growth of the prior layer is finished. The granular borders may be seen clearly [13, 19-21]. If it is noticed that the average particle size is large in the sample (CCTS), then it begins to decrease and rise as a result of the temperature difference.

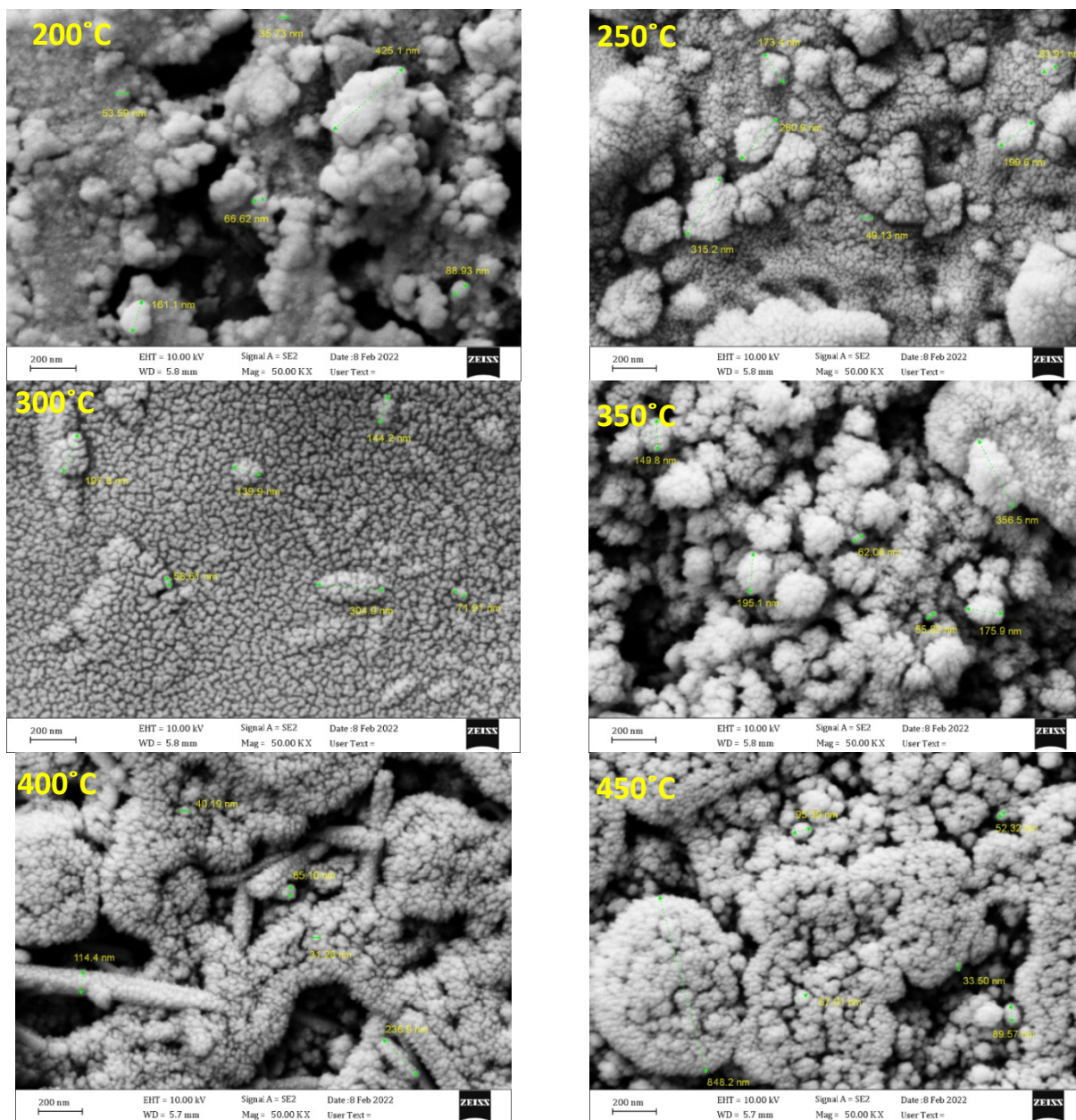


Figure 3. FESEM micro-images of CCTS samples deposited at different temperatures

The optical characteristics of the CCTS films were examined through the absorbance (*A*) of UV-visible spectra. The absorption coefficient (α) of any film of thickness (*t*) could be calculated using the following relationship [22]:

$$\alpha = 2.303 A/t, \tag{5}$$

The values of α were found to be greater than 10^4 cm^{-1} . Using Tauc's formula, the optical band gap, E_g , could be evaluated from the absorption spectra [23]:

$$(\alpha E) = P(E - E_g)^r, \tag{6}$$

where *P* is constant, *E* stands for photon energy, while *r* is an empirical quantity that describes the electronic transition type which is equal to 1/2 for direct allowed transition.

In this study, a straight line was generated by sketching a plot between $(\alpha E)^2$ and (*E*). The direct bandgap could then be estimated by extrapolating this straight line to $(\alpha h\nu)^2 = 0$, as shown in Figure 4. The estimated values of E_g were in

the range of 1.69-1.95 eV. This matches well with the findings of other reports [24, 25]. Because of the unsaturated bonds and/or micro-stress generated during the growth which leads to local states of high density, there may be a variance in the energy gap value [7].

In order to define the electrical characteristics of the CCTS films, the Hall Effect was carried out to ascertain the type, concentration, mobility, and conductivity of majority charge carriers. The results of this test are shown in Table 3, which shows positive values of R_H (p-type) consistent with the findings of earlier investigations [4].

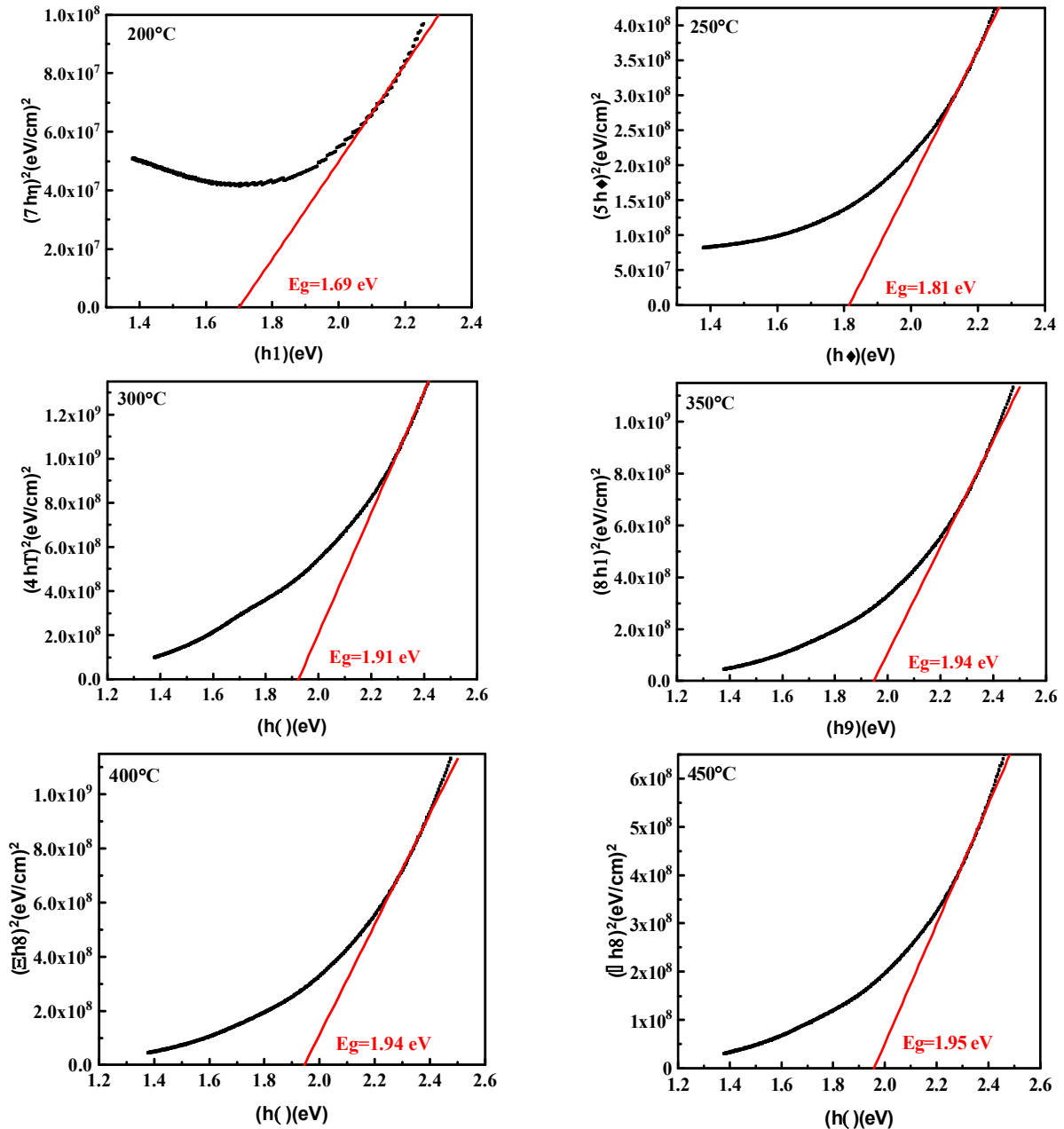


Figure 4. Energy gap of CCTS films prepared at different temperatures

Table 3. Outcomes of Hall Effect test of CCTS samples

Temperature (°C)	Hall coef. (cm^3/C)	Concentration (cm^{-3}) $\times 10^{17}$	Mobility ($\text{cm}^2/\text{V.s}$)	Resistivity ($\Omega.\text{cm}$)	Conductivity ($\Omega.\text{cm}$) ⁻¹
200	15.19	4.11	3.026	5.019	0.199
250	11.96	5.22	4.551	2.627	0.380
300	8.53	7.32	5.213	1.636	0.611
350	6.75	9.25	6.011	1.123	0.890
400	7.79	8.01	5.337	1.46	0.685
450	10.32	6.05	4.002	2.578	0.387

The electrical conductivity, mobility, and concentration of charge carriers have increasing trend as the deposition temperature is increased upto 350 °C, and then they began to decline, as shown in Figures 5 and 6. The results of XRD analysis support this [17].

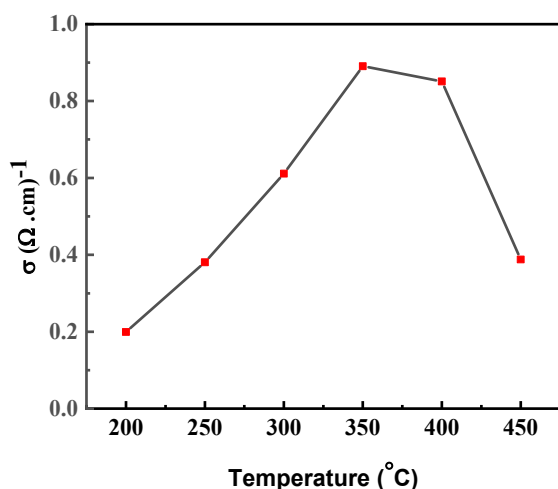


Figure 5. Hall conductivity of CCTS films at various temperatures

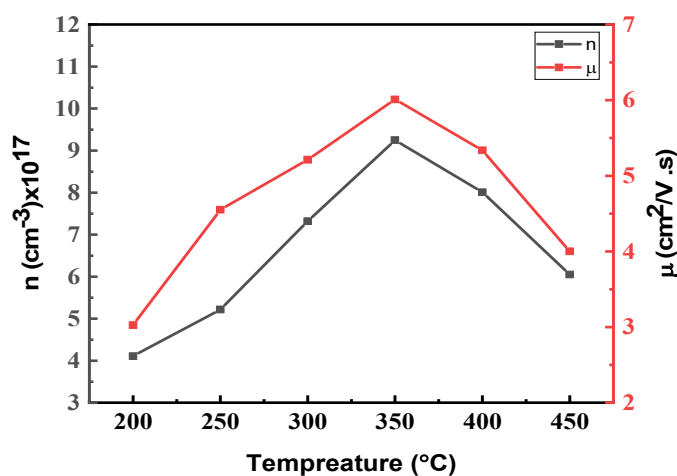


Figure 6. Charge carriers and their mobility of CCTS films at various temperatures

CONCLUSIONS

According to XRD observations, the CCTS films were found to be tetragonal polycrystalline having favorable growth direction of (112). The quaternary CCTS compound's high and distinct peaks at (335, 336, and 337 cm^{-1}) were revealed by Raman spectroscopy, supporting the XRD findings. Different grain sizes and shapes could be seen in the micro-images obtained by FESEM. Electrical measurements of the Hall Effect show that the conductivity was p-type. The band gap range (1.69-1.95 eV) as well as the coefficient of optical absorption (10^4 cm^{-1}) are extremely near to the optimal material values employed in the absorbent layer in solar cells.

ORCID IDs

© Huda Talib, <https://orcid.org/0000-0001-6285-9978>; © Nabeel A. Bakr, <https://orcid.org/0000-0002-8819-5847>;
© Mohammed A. Abed, <https://orcid.org/0000-0001-5091-0721>

REFERENCES

- [1] S. Vanalakar, P. Patil, and J. Kim, "Recent advances in synthesis of $\text{Cu}_2\text{FeSnS}_4$ materials for solar cell applications: A review", *Solar Energy Materials and Solar Cells*, **182**, 204-219 (2018). <https://doi.org/10.1016/j.solmat.2018.03.021>
- [2] J. Trajic, M. Romcevic, M. Petrovic, M. Gilic, P. Balaz, A. Zorkovska, and N. Romcevic, "Optical properties of the mechanochemically synthesized $\text{Cu}_2\text{FeSnS}_4$ (stannite) nanocrystals: Raman study", *Optical Materials*, **75**, 314-318 (2018). <https://doi.org/10.1016/j.optmat.2017.10.043>
- [3] M. Cao, C. Li, B. Zhang, J. Huang, L. Wang, and Y. Shen, "PVP assisted solvothermal synthesis of uniform $\text{Cu}_2\text{FeSnS}_4$ nanospheres", *Journal of Alloys and Compounds*, **622**, 695-702 (2015). <https://doi.org/10.1016/j.jallcom.2014.10.164>
- [4] M. Adelifard, "Preparation and characterization of $\text{Cu}_2\text{FeSnS}_4$ quaternary semiconductor thin films via the spray pyrolysis technique for photovoltaic applications", *Journal of Analytical and Applied Pyrolysis*, **122**, 209-215 (2016). <https://doi.org/10.1016/j.jaap.2016.09.022>
- [5] Z.T. Khodair, N.A. Bakr, A. M. Hassan, and A.A. Kamil, "Influence of Substrate temperature and thickness on structural and optical properties of CZTS nanostructures thin films", *Journal of Ovonic Research*, **15**, 377-385 (2019).
- [6] M.A. Abed, N.A. Bakr, and S.B. Mohammed, "Synthesis and Characterization of Chemically Spayed $\text{Cu}_2\text{FeSnS}_4$ (CTFS) Thin Films: The Effect of Substrate Temperature", *Materials Science Forum*, **1039**, 434-441 (2021). <https://doi.org/10.4028/www.scientific.net/MSF.1039.434>
- [7] M.A. Abed, N.A. Bakr, and J. Al-Zanganawee, "Structural, Optical and Electrical Properties of $\text{Cu}_2\text{NiSnS}_4$ Thin Films Deposited by Chemical Spray Pyrolysis Method", *Chalcogenide Letters*, **17**, 179-186 (2020).
- [8] S.G. Nilange, N.M. Patil, and A.A. Yadav, "Growth and characterization of spray deposited quaternary $\text{Cu}_2\text{FeSnS}_4$ semiconductor thin films.", *Physica B: Condensed Matter*, **560**, 103-110 (2019). <https://doi.org/10.1016/j.physb.2019.02.008>
- [9] M. Benchikri, O. Zaberca, R. El Ouatib, B. Durand, F. Oftinger, A. Balocchi, and J.Y. Chane-Ching, "A high temperature route to the formation of highly pure quaternary chalcogenide particles", *Mater. Lett.* **68**, 340-343 (2012). <https://doi.org/10.1016/j.matlet.2011.10.105>
- [10] W. Daranf, M.S. Aida, A. Hafidallah, and H. Lekiket, "Substrate temperature influence on ZnS thin films prepared by ultrasonic spray", *Thin Solid Films*, **518**, 1082-1084 (2009). <https://doi.org/10.1016/j.tsf.2009.03.227>
- [11] H. Hussein, and A. Yazdani, "Spin-coated $\text{Cu}_2\text{CrSnS}_4$ thin film: A potential candidate for thin film solar cells", *Materials Science in Semiconductor Processing*, **91**, 58-65 (2019). <https://doi.org/10.1016/j.mssp.2018.11.005>
- [12] A. Sharma, P. Sahoo, A. Singha, S. Padhan, G. Udayabhanu, and R. Thangavel, "Efficient visible-light-driven water splitting performance of sulfidation-free, solution processed $\text{Cu}_2\text{MgSnS}_4$ thin films: role of post-drying temperature", *Solar Energy*, **203**, 284-295 (2020). <https://doi.org/10.1016/j.solener.2020.04.027>

- [13] S. Dridi, N. Bitri, and M. Abaab, "Synthesis of quaternary Cu₂NiSnS₄ thin films as a solar energy material prepared through «spray» technique", *Materials Letters*, **204**, 61–64 (2017). <https://doi.org/10.1016/j.matlet.2017.06.028>
- [14] H.J. Ahmed, A.A. Kamil, A.A. Habeeb, and N.A. Bakr, "The influence of Deposition Temperature on the Properties of Chemically Sprayed Nanostructured Cu₂CdSnS₄ Thin Films", *International Research Journal of Science and Technology*, **1**, 149-155 (2020). <https://doi.org/10.46378/irjst.2020.010211>
- [15] D. Fikri, A. Yuwono, N. Sofyan, T. Arini, and L. Lalasari, "The effect of substrate heating temperature upon spray pyrolysis process on the morphological and functional properties of fluorine tin oxide conducting glass", *AIP Conference Proceedings*, **1826**, 1–9 (2017). <https://doi.org/10.1063/1.4979219>
- [16] R.R. Prabhakar, N.H. Loc, M.H. Kumar, P.P. Boix, S. Juan, R.A. John, S.K. Batabyal, and L.H. Wong, "Facile water-based spray pyrolysis of earth-abundant Cu₂FeSnS₄ thin films as an efficient counter electrode in dye-sensitized solar cells", *ACS applied materials & interfaces*, **20**, 17661–17667 (2014). <https://doi.org/10.1021/am503888v>
- [17] C. Dong, G.Y. Ashebir, J. Qi, J. Chen, Z. Wana, W. Chen, and M. Wang, "Solution-processed Cu₂FeSnS₄ thin films for photovoltaic application", *Materials Letters*, **214**, 287-289 (2018). <https://doi.org/10.1016/j.matlet.2017.12.032>
- [18] C. Yan, C. Huang, J. Yang, F. Liu, J. Liu, Y. Lai, J. Lib, and Y. Liua, "Synthesis and characterizations of quaternary Cu₂FeSnS₄ nanocrystals", *Chemical Communications*, **20**, 2603-2605 (2012). <https://doi.org/10.1039/C2CC16972J>
- [19] J. M. Pawlikowski, "Preparation and characterization of close-spaced vapour transport thin films of ZnSe for heterojunction solar cells", *Thin Solid Films*, **127**, 9-28 (1985). [https://doi.org/10.1016/0040-6090\(85\)90209-3](https://doi.org/10.1016/0040-6090(85)90209-3)
- [20] W.H. Koschel, F. Sorger, and J. Baars, "Optical phonons in I-III-VI₂ compounds", *Le Journal De Physique Colloques*, **36**, C3-177-C3-181 (1975). <https://doi.org/10.1051/jphyscol:1975332>
- [21] P.S. Maldar, M.A. Gaikwad, A.A. Mane, S.S. Nikam, S.P. Desai, A. Sarkar, and A.V. Moholkar, "Fabrication of Cu₂CoSnS₄ thin films by a facile spray pyrolysis for photovoltaic application." *Solar Energy*, **158**, 89-99 (2017). <https://doi.org/10.1016/j.solener.2017.09.036>
- [22] N.A. Bakr, Z.T. Khodair, and H.I. Mahdi, "Influence of Thiourea Concentration on Some Physical Properties of Chemically Sprayed Cu₂ZnSnS₄ Thin Films", *International Journal of Materials Science and Applications*, **5**, 261-270 (2016). <https://doi.org/10.11648/j.ijmsa.20160506.15>
- [23] S.A. Hameed, N.A. Bakr, A.M. Hassan, and A.N. Jasim, "Structural and optical properties of Cu₂ZnSnS₄ thin films fabricated by chemical spray pyrolysis", *AIP Conference Proceedings*, **2213**, 10.1063-5.0000316 (2020). <https://doi.org/10.1063/5.0000310>
- [24] A. Ghosh, A. Biswas, R. Thangavel, and G. Udayabhana, "Photo-electrochemical properties and electronic band structure of kesterite copper chalcogenide Cu₂-II-Sn-S₄ (II = Fe, Co, Ni) thin films", *RSC Advances*, **6**, 96025-96034 (2016). <https://doi.org/10.1039/C6RA15700A>
- [25] S. Lee, J. Kim, H. Woo, Y. Jo, A. Inamdar, S. Pawar, H. Kim, W. Jung, and H. Im, "Structural, morphological, compositional, and optical properties of single step electrodeposited Cu₂ZnSnS₄ (CZTS) thin films for solar cell application", *Current Applied Physics*, **14**, 254-258 (2014). <https://doi.org/10.1016/j.cap.2013.11.028>

ОТРИМАННЯ ТА ХАРАКТЕРИСТИКА ТОНКИХ ПЛІВОК CU₂CrSnS₄, НАНЕСЕНИХ ПРИ РІЗНИХ ТЕМПЕРАТУРАХ

Худа Таліб^{a,b}, Набіл А. Бакр^a, Мохаммед А. Абед^b

^aФакультет фізики, Науковий коледж, Університет Діяла, Діяла, Ірак

^bГоловне управління освіти Діяла, Діяла, Ірак

У цьому дослідженні тонкі плівки Cu₂CrSnS₄ отримані за допомогою техніки хімічного піролізу при різних температурах осадження (200, 250, 300, 350, 400 і 450°C) і без будь-якого процесу відпалювання. Структурні характеристики плівок були вивчені за допомогою дифракції рентгенівських променів (XRD), мікро-Раманівської спектроскопії та польово-емісійного скануючого електронного мікроскопа (FESEM), тоді як оптичні характеристики досліджені за допомогою УФ-видимої спектrophотометрії, а також описані електричні властивості за допомогою тесту на ефект Холла. Результати XRD для плівок Cu₂CrSnS₄ (CCTS) показали тетрагональну кристалічну структуру станичної фази з переважною орієнтацією (112). Результати раманівської спектроскопії підготовлених тонких плівок CCTS показали чіткий пік при ~ 336 см⁻¹. Крім того, результати морфології та наскрізні (FESEM) зображення поверхні тонких плівок показали різні форми та форми з різним розміром зерен у діапазоні від 40 до 294 нм. Оптичне дослідження ультрафіолетового та видимого спектру показало оптичний енергетичний проміжок (1,69-1,59 eV), який вважається придатним для застосування в тонкоплівкових сонячних елементах. Електричні вимірювання за допомогою тесту на ефект Холла показали, що плівки мають носії заряду (p-типу). З аналізу результатів оптимізована температура підготовлених (CCTS) зразків становила 350°C.

Ключові слова: Cu₂CrSnS₄, розпилувальний піроліз, температура осадження, рентгеноструктурний аналіз, УФ-видима спектроскопія, ефект Холла